Barium Cloud Density Variation in a Highly-Conducting Background.

ROCHESTER UNIV NY

MAR 1971

UNCLASSIFIED
Security Classification

DOCUMENT CONTROL DATA - R & D

(Security classification of title, body of abstract and indexing annotation must be entered when the overall report is classified)

1. ORIGINATING ACTIVITY (Corporate author)
University of Rochester
River Campus
Rochester, NY 14627

2a. REPORT SECURITY CLASSIFICATION
UNCLASSIFIED

2b. GROUP

3. REPORT TITLE
Barium Cloud Density Variation in a Highly-Conducting Background

4. DESCRIPTIVE NOTES (Type of report and inclusive dates)
Semi-Annual Technical Report 15 Sept 70 - 14 Mar 71

5. AUTHOR(S) (First name, middle initial, last name)
Albert Simon
Arthur M. Sleeper

6. REPORT DATE
March 1971

7a. TOTAL NO. OF PAGES
20

7b. NO. OF REFS
2

8a. CONTRACT OR GRANT NO.
F30602-70-C-0001

b. PROJECT NO.
ARPA Order 1057

c. Program Code Number 0E20

d.

9a. ORIGINATOR'S REPORT NUMBER(S)

9b. OTHER REPORT NO(S) (Any other numbers that may be assigned this report)

10. DISTRIBUTION STATEMENT This document is subject to special export controls and each transmittal to foreign governments or foreign nationals may be made only with prior approval of ARPA, Arlington VA 22209

11. SUPPLEMENTARY NOTES Monitored by:
RADC/OCSE (L. Strauss)
Griffiss AFB NY 13440

12. SPONSORING MILITARY ACTIVITY
Advanced Research Project Agency
1400 Wilson Blvd
Arlington VA 22209

13. ABSTRACT

An equation is derived for the growth in time of a barium cloud in a strongly conducting background. The expression is correct to first order in an expansion in powers of the ratio of the cross-cloud conductivity to the background conductivity. Numerical solutions of this equation indicate significant differences from the zero order result. There is steepening of the backside of the cloud and elongation in the E X B direction.

The list of weakly ionized instabilities is extended to include the true gravitational instability. This is the closest contender to the E X B but still appears to have a threshold higher by about a factor of ten.

DD FORM 1 NOV 65 1473

UNCLASSIFIED
Security Classification

14. KEY WORDS	LINK A		LINK B		LINK C	
	ROLE	WT	ROLE	WT	ROLE	WT
Barium Clouds						
E X B Instability						
Gravitational Instability						

BARIUM CLOUD DENSITY VARIATION IN A HIGHLY-CONDUCTING BACKGROUND

Albert Simon
Arthur M. Sleeper

University of Rochester

This research was supported by the Advanced Research Projects Agency of the Department of Defense and was monitored by Leonard Strauss RADC (OCSE), GAFB, NY 13440 under Contract F30602-70-C-0001.

PUBLICATION REVIEW

This technical report has been reviewed and is approved.

Vincent J Coyne
RADC Project Engineer

Leonard C Haus
RADC Contract Engineer

ABSTRACT

An equation is derived for the growth in time of a barium cloud in a strongly conducting background. The expression is correct to first order in an expansion in powers of the ratio of the cross-cloud conductivity to the background conductivity. Numerical solutions of this equation indicate significant differences from the zero order result. The forward moving part of the cloud thins and indents while the backside steepens.

The list of weakly ionized instabilities is extended to include the true gravitational instability. This is the closest contender to the E X B but still appears to have a threshold higher by about a factor of ten.

TABLE OF CONTENTS

LIST OF ILLUSTRATIONS

I. INTRODUCTION

In the previous semi-annual technical reports[1,2] we have discussed the various instabilities which a low-β , weakly-ionized plasma is subject to and demonstrated that the threshold for onset of the $\underset{\sim}{E} \times \underset{\sim}{B}$ instability is lower than for all others. In order to further identify the instability, it is necessary to develop a realistic model of the equilibrium state of the cloud just before onset of striation. A model sufficient for this purpose was developed and reported in I. Linearization of the equations of motion about this equilibrium state then provides a convenient set of equations for numerical calculation. Some of the results obtained were reported in II. Further results are noted in Section IV of this report. We are now designing an improved numerical scheme which will allow considerable increase in grid size and should advance our knowledge of the critical eigenvalues and eigenstates.

In the meantime emphasis has shifted, for the moment, to extending the model of the equilibrium state. The previous model assumed a background ionosphere which was infinitely conducting. This meant that there was no dielectric reduction of the ambient electric field in the interior of the cloud due to charges collecting on the surface. As a result the cloud moved smoothly (gaussian density distribution) and with a velocity equal to that of the ions alone (modified only by the internal ambipolar electric field). We have now extended this model to include the first order correction in an expansion in powers of the small ratio of the cross-cloud conductivity to the ionosphere's

conductivity. This extension allows dielectric screening of the external field to occur. Time-dependent numerical solutions of these modified equilibrium equations give evidence of flattening of the rear of the cloud and indentation and thinning in the direction of drift.

The extended equilibrium model is discussed in Section II below. Numerical results are given in Section III. A brief discussion of the instability eigenvalue calculations is in Section IV as well as extension of previous instability estimates to include the "true" gravitational instability.

II. EQUILIBRIUM STATE IN A HIGHLY-CONDUCTING BACKGROUND

In the rest frame of the neutrals, the equation of motion of the barium plasma takes the form

$$\partial N/\partial t - D_\perp^\pm \nabla_\perp^2 N - D_{11}^\pm \nabla_{11}^2 N \pm \mu_\perp^\pm \underline{\nabla}_\perp \cdot (N \underline{E}_\perp)$$

$$\pm \mu_{11}^\pm \nabla_{11} (N E_{11}) + (\Omega\tau)^\pm \mu_\perp^\pm \underline{b} \cdot \underline{\nabla} N \times \underline{E} = 0 \qquad (1)$$

where the symbols all have the same meaning as in I. If one now subtracts the electron form of Equation (1) from the ion form, we obtain

$$-(D_\perp^+ - D_\perp^-) \nabla_\perp^2 N + (D_{11}^- - D_{11}^+) \nabla_{11}^2 N + (\mu_\perp^- + \mu_\perp^+) \underline{\nabla}_\perp \cdot (N \underline{E})$$

$$+ (\mu_{11}^- + \mu_{11}^+) \nabla_{11} (N E_{11}) - \left((\Omega\tau)^- \mu_\perp^- - (\Omega\tau)^+ \mu_\perp^+ \right) \underline{b} \cdot \underline{\nabla} N \times \underline{E} = 0 \qquad (2)$$

In the equilibrium state we assume a smooth profile with characteristic length r and l in the radial and parallel direction of the order of $r^2/l^2 \cong D_\perp^+ / D_{11}^+$ and with $E_\perp \cong -\phi/r + E_o$, $E_{11} \cong -\phi/l$ where E_o is the ambient electric field in the neutral rest frame. We also assume $e\phi \cong KT$ where T denotes the common temperature. Dividing all terms by D_{11}^-/l^2 and using the Einstein relations and the usual inequalities $(\Omega\tau)_-^2 >> (\Omega\tau)_+^2$, $\mu_{11}^- >> \mu_{11}^+$, $D_\perp^+ >> D_\perp^-$ it is easy to see that all terms in Equation (2) except for the second and fourth are of order $D_{11}^+ / D_{11}^- << 1$. We assume $e E_o l / KT$ of order ten or less and thus not

large enough to change the ordering due to $D_{\perp}^{+}/D_{\parallel}^{-}$ which is approximately (1/1300). We also assume ν and ℓ of similar order and $(\Omega\tau)_{+}$ of order unity or larger.

To lowest order in an expansion in powers of $D_{\parallel}^{+}/D_{\parallel}^{-}$ our equation becomes:

$$\nabla_{\parallel}\left[A\,\nabla_{\parallel}N + N E_{\parallel}\right] = 0$$

where

$$A = D_{\parallel}^{-}/\mu_{\parallel}^{-} = kT^{-}/e \tag{3}$$

Integration yields

$$A\,\nabla_{\parallel}N + N E_{\parallel} + \gamma(\underset{\sim}{\Omega}_{\perp}) = 0\,. \tag{4}$$

Assuming symmetry of the equilibrium about the $z=0$ plane, we have $\gamma = 0$. Integrating once more yields

$$A \ln N - \phi + \vartheta(\underset{\sim}{\Omega}_{\perp}) = 0 \tag{5}$$

Unlike the method used in I, we shall confine our expansion in $D_{\parallel}^{+}/D_{\parallel}^{-}$ to the lowest order, so that Equation (5) is our basic equation for determining E. However, again unlike I, we will not assume an infinitely conducting background but will use the following improved method to determine $\vartheta(\underset{\sim}{\Omega}_{\perp})$.

By our general assumption of quasineutrality, we must have

$$\underset{\sim}{\nabla}\cdot\underset{\sim}{J} = 0 \tag{6}$$

at every point in space, where $\underset{\sim}{J}$ denotes the electrical current. If we now integrate Equation (6) along a magnetic field line passing through the cloud, from a point infinitely far from the cloud on one side to a similar point on the other side, and use the vanishing of the parallel flux at infinity, one obtains

$$\int_{CLOUD} \nabla_\perp \cdot \underline{J}_\perp \, dz = - \int_{IONO} \nabla_\perp \cdot \underline{J}_\perp \, dz \qquad (7)$$

Here we have separated the surviving terms into a portion integrated over the cloud and that integrated over the ionosphere. By Equation (5), we see that the perpendicular electric field is independent of z outside the cloud (Note that $\ln N$ is constant outside the cloud). As a result, the r.h.s. of Equation (7) may be written as

$$- \int_{IONO} \sigma_p \, \nabla_\perp \cdot \underline{E}_\perp \, dz$$

or

$$- \Sigma_B \, \nabla_\perp \cdot \underline{E}_\perp$$

where σ_p is the Pedersen conductivity in the ionosphere and Σ_B is its height integral.

We thus obtain the equation

$$\nabla_\perp \cdot \underline{E}_\perp = - \frac{1}{\Sigma_B} \int_{CLOUD} \nabla_\perp \cdot \underline{J}_\perp \, dz \, . \qquad (8)$$

The integral on the r.h.s. is proportional to σ_c, the characteristic cross field conductivity of the cloud, and thus the right hand side is proportional to $\sigma_c a / \Sigma_B$ where a is a characteristic width of the cloud. We assume that the cross field conductivity in region B is very large compared to the cloud conductivity, hence this parameter is small. If one now expands $\underline{E}_\perp$ in powers of λ $\left(\lambda \equiv \sigma_c a / \Sigma_B\right)$ one immediately obtains the zero-order solution $\nabla_\perp \cdot \underline{E}_\perp^{(o)} = 0$.

Since the external field must be equal to the ambient field far from the cloud, this yields $\underline{E}_\perp^{(o)} = \underline{E}_o$.

We now use this result to calculate $\underline{E}$ in the cloud, and then N in the cloud. By Equation (5)

$$\phi = A \ln N + g(\underset{\sim}{r}_\perp)$$

$$\therefore \quad \underset{\sim}{E}^{(c)} = -\frac{A \nabla N}{N} + \underset{\sim}{E}_0 \tag{9}$$

where we assume the first term vanishes outside the cloud. Now substitute Equation (9) in the fourth and sixth terms of Equation (1) and then eliminate the fifth term by the appropriate combination of the ion and electron forms of Equation (1). The result is:

$$\frac{\partial N}{\partial t} - \mathcal{D}_{11} \nabla_{11}^2 N - \mathcal{D}_\perp \nabla_\perp^2 N + (1-\alpha) \frac{c}{B} \underset{\sim}{E}_0 \times \underset{\sim}{b} \cdot \nabla N$$

$$+ \frac{c\beta}{B} (\underset{\sim}{E}_0 \nabla) N = 0 \tag{10}$$

This equation is identical to Equation (12) of I if one transforms to the frame moving with velocity $\underset{\sim}{u}_c = c \underset{\sim}{E}_0 \times \underset{\sim}{b} / B$. All symbols have the same meaning as in this equation. Thus the solution for N follows immediately from Equation (13) of I and is:

$$N(\underset{\sim}{r}, t) = \frac{S_0}{4\pi \mathcal{D}_\perp t \, (4\pi \mathcal{D}_{11} t)^{\frac{1}{2}}} \times$$

$$\times \exp \left\{ - \frac{[\underset{\sim}{r}_\perp + (\alpha - 1) \underset{\sim}{u}_c t + \beta \underset{\sim}{u}_c \times \underset{\sim}{b} t]^2}{4 \mathcal{D}_\perp t} - \frac{z^2}{4 \mathcal{D}_{11} t} \right\} . \tag{11}$$

assuming an impulse source of strength S_0 at the origin at $t = 0$.

The fact that the resulting density distribution is identical with that in I is not surprising since to lowest order in λ, the background ionosphere appears to be infinitely conducting (relative to the cross cloud conductivity). It is also

no surprise that the cloud is cylindrically symmetric since there can be no dielectric distortion in this same approximation. (The only charge that can build up on the outer surface of the cloud is one that is uniform over the entire surface.) This is the nature of the ambipolar field specified by the first term in Equation (9). Note that $\underset{\sim}{E}_\perp$ is a constant along the field lines, as assumed.

Let us now proceed to first order in λ. Equation (8) becomes

$$\nabla_\perp \cdot \underset{\sim}{E}_\perp^{(1)} = -\frac{1}{\Sigma_B} \int_{CLOUD} \nabla_\perp \cdot \underset{\sim}{J}_\perp^{(0)} dz \,.$$

The zero-order current is obtained at once by using the usual diffusion expression together with Eqs. (9) and (11). The result takes a particularly simple form if one makes the formal transformation

$$\begin{aligned} \underset{\sim}{r}' &= \underset{\sim}{r} + (\alpha - 1)\, \underset{\sim}{u}_0 t + \beta\, \underset{\sim}{u}_0 \times \underset{\sim}{b}\, t \\ t' &= t \,. \end{aligned} \tag{12}$$

In terms of these coordinates the expression above takes the form

$$\nabla_\perp^2 \phi^{(1)} = \frac{-e S_0 \pi}{\Sigma_B (4\pi \mathcal{D}_\perp t)^2} \left\{ \frac{r_\perp^2 - 4\mathcal{D}_\perp t}{t} + \right.$$

$$\left. - \frac{2B}{c} \mu_\perp^+ \left[(\Omega\tau)_+^{-1} \underset{\sim}{u}_0 \cdot \underset{\sim}{r} + \underset{\sim}{u}_0 \times \underset{\sim}{b} \cdot \underset{\sim}{r} \right] \right\} \times$$

$$\times \exp\left(\frac{-r_\perp^2}{4\mathcal{D}_\perp t} \right) . \tag{13}$$

where we have omitted the primes, set $\underset{\sim}{E}_\perp^{(1)} = -\nabla_\perp \phi^{(1)}$ and assumed $(\Omega\tau)_- \to \infty$. The boundary condition is that $\underset{\sim}{E}_\perp^{(1)}$ vanish far from the cloud.

Using the Green's function method, the solution is:

$$\phi^{(1)}(\underset{\sim}{r},t) = \frac{1}{2\pi}\int \ln R \cdot \chi(\underset{\sim}{r}',t)\, d^2 r_\perp'$$

where $\underset{\sim}{R} = \underset{\sim}{r}_\perp - \underset{\sim}{r}_\perp'$ and χ denotes the r.h.s. of Equation (13). Using the well-known expansion (see Morse and Feshbach, Equation (10.1.18)

$$\ln R = \ln \rho_> - \sum_{m=1}^{\infty} \frac{1}{m}\left(\frac{\rho_<}{\rho_>}\right)^m \cos\left[m(\phi-\phi')\right]$$

where $\rho_>$ is the greater of $r_\perp$ and $r_\perp'$ and $\rho_<$ is the lesser, it is easy to carry out the angular integral. The result is:

$$\phi^{(1)} = \frac{-e S_0}{\pi \Sigma_B (4D_\perp t)^2}\int_0^\infty \left\{ \frac{r'^2 - 4D_\perp t}{t} \ln \rho_> + \right.$$

$$\left. + \frac{B}{c}\mu_\perp^+ \left[(\Omega\tau)_+^{-1}\underset{\sim}{u}_0\cdot\underset{\sim}{r} + \underset{\sim}{u}_0 \times \underset{\sim}{b}\cdot\underset{\sim}{r}\right]\frac{r'}{r}\cdot\frac{\rho_<}{\rho_>}\right\} \exp\left(\frac{-r'^2}{4D_\perp t}\right) r'\,dr'.$$

One can now calculate most of the remaining integrals with the result

$$\phi^{(1)} = \frac{-e S_0}{\pi \Sigma_B (4D_\perp t)^2}\left\{ \ln r \int_0^r \left(\frac{r'^2 - 4D_\perp t}{t}\right)\exp\left(\frac{-r'^2}{4D_\perp t}\right) r'\,dr' \right.$$

$$+ \int_r^\infty \left(\frac{r'^2 - 4D_\perp t}{t}\right)\ln r' \exp\left(\frac{-r'^2}{4D_\perp t}\right) r'\,dr'$$

$$+ \frac{B}{c}\mu_\perp^+\left[(\Omega\tau)_+^{-1}\underset{\sim}{u}_0\cdot\underset{\sim}{r} + \underset{\sim}{u}_0\times\underset{\sim}{b}\cdot\underset{\sim}{r}\right]\frac{8(D_\perp t)^2}{r^2} \times$$

$$\left. \times \left(1 - \exp\left(-\frac{r^2}{4D_\perp t}\right)\right)\right\}.$$

The resulting electric field follows by differentiation. We obtain

$$\underline{E}^{(1)} = \frac{-eS_0}{\pi \Sigma_B (4D_\perp t)^2} \left\{ -\frac{\underline{i}_r}{r} \int_0^r \left(\frac{r'^2 - 4D_\perp t}{t} \right) EXP\left(-\frac{r'^2}{4D_\perp t} \right) r' dr' \right.$$

$$- \frac{B}{c} \mu_\perp^+ \left[(\Omega\tau)_+^{-1} \underline{u}_0 + \underline{u}_0 \times \underline{b} \right] \frac{8(D_\perp t)^2}{r^2} \left[1 - EXP\left(\frac{-r^2}{4D_\perp t} \right) \right]$$

$$+ \frac{B}{c} \mu_\perp^+ \left[(\Omega\tau)_+^{-1} \underline{u}_0 \cdot \underline{r} + \underline{u}_0 \times \underline{b} \cdot \underline{r} \right] \frac{16(D_\perp t)^2}{r^3} \underline{i}_r \times$$

$$\left. \times \left[1 - (1 + r^2/4D_\perp t) EXP(-r^2/4D_\perp t) \right] \right\}.$$

$$= \frac{-eS_0}{2\pi \Sigma_B r^2} \left\{ \underline{i}_r \left(\frac{r^3}{4D_\perp t^2} EXP\left(-\frac{r^2}{4D_\perp t} \right) + \right. \right.$$

$$\left. + \frac{B}{c} \mu_\perp^+ \left[(\Omega\tau)_+^{-1} \underline{u}_0 \cdot \underline{r} + \underline{u}_0 \times \underline{b} \cdot \underline{r} \right] \frac{2}{r} \left[1 - \left(1 + \frac{r^2}{4D_\perp t} \right) EXP\left(-\frac{r^2}{4D_\perp t} \right) \right] \right)$$

$$\left. - \frac{B}{c} \mu_\perp^+ \left[(\Omega\tau)_+^{-1} \underline{u}_0 + \underline{u}_0 \times \underline{b} \right] \left[1 - EXP\left(-\frac{r^2}{4D_\perp t} \right) \right] \right\}.$$

(14)

where $\underset{\sim}{\epsilon}_r$ is a unit vector in the radial direction. The obvious extension of Equation (9) is

$$\underset{\sim}{E} = -A\frac{\nabla N}{N} + \underset{\sim}{E}_0 + \underset{\sim}{E}^{(1)} \tag{15}$$

If we also transform Equation (1) to the coordinates expressed by Equation (12), substitute Equation (15) in the fourth and sixth terms and eliminate the fifth term between the electron and ion forms of this equation, the result is

$$\frac{\partial N}{\partial t} - \mathcal{D}_{11}\nabla_{11}^2 N - \mathcal{D}_{\perp}\nabla_{\perp}^2 N + \frac{c}{B}\beta\,\nabla_{\perp}\cdot(N\underset{\sim}{E}^{(1)})$$

$$+ \frac{c}{B}(1-\alpha)\,\underset{\sim}{b}\cdot\nabla N\times\underset{\sim}{E}^{(1)} = 0 \tag{16}$$

where $\underset{\sim}{E}^{(1)}$ is given by Equation (14). This is the equation of motion of the ion density as seen from a frame moving relative to the neutrals with the transformation given by Equation (12), i.e...a frame moving with the velocity of the cloud in an infinitely conducting background.

III. NUMERICAL SOLUTION FOR TIME DEVELOPMENT OF THE EQUILIBRIUM STATE

Equation (16) is reduced to two-dimensional form by averaging over the z-direction. Thus Equation (16) reduces to

$$\partial N/\partial t - D_\perp \nabla_\perp^2 N + \frac{c}{B}\beta \nabla_\perp \cdot (N \underset{\sim}{E}^{(1)}) + \frac{c}{B}(1-\alpha)\underset{\sim}{b}\cdot \nabla N \times \underset{\sim}{E}^{(1)} = 0 \qquad (17)$$

where $N = N(\underset{\sim}{r}_\perp, t)$. A computer solution is then obtained by assuming an initial solution

$$N(0) = \frac{S_0}{\pi a^2} e^{-r^2/a^2}$$

measuring all lengths in terms of a and time in units of $a^2/4D_\perp$ (The proper value of $\underset{\sim}{E}^{(1)}$ is then given by Equation (14) with t replaced by $(t + a^2/4D_\perp)$.) Two basic dimensionless parameters also appear in the dimensionless form of Equation (17). These are:

$$\bar{\lambda} = \frac{e S_0 \mu_\perp^+}{\pi \Sigma_p a^2}$$

which is the ratio of the cross-cloud conductivity to that of the background and

$$\gamma = \frac{e E_0 a}{K(T_+ + T_-)}$$

which is the normalized external electric field strength. The solution is obtained by a difference scheme using the A.D.I. method. Further details will be given in a separate report.

Typical results are shown in Figures 1-5. Here one chose

$$a = 4.8 \text{ KM}$$

$$D_\perp = .045 \ (\text{KM})^2/\text{SEC}$$

and the length scale is then shown in units of kilometers. The magnetic field is out of the paper and $\underset{\sim}{E}_o$ is in the positive y- direction. Note the interesting distortion which occurs in time. The rear of the cloud tends to flatten and steepen, while the front side indents and thins. All these results have a simple interpretation in terms of the polarization produced in the cloud by Pedersen currents (as well as Hall currents at low $(\Omega\tau)_+$).

IV. OTHER WORK IN PROGRESS

The numerical scheme for evaluating the stability boundaries and for determining the shape of the eigenfunctions is being completely revised. The previous method, described in II, was pushed to an 11x11 grid size with no significant change in the general form of the results. Now we plan to use a much faster method which yields only the most rapidly growing eigenvalue, instead of all eigenvalues. Advice and assistance is being obtained from the Los Alamos Scientific Laboratory.

The catalog of low frequency instabilities in weakly ionized plasma was examined in I to determine the most likely candidate for the origin of barium cloud striation. The $\underset{\sim}{E} \times \underset{\sim}{B}$ was shown to have a threshold about a factor of 100 lower than that for the ion sound instability (either $\underset{\sim}{E} \times \underset{\sim}{B}$ driven or driven by diamagnetic streaming) or the drift dissipative instability. The gravitational instability due to magnetic field curvature is negligible compared to the above; however the "true" gravitational instability is a serious contender.* We have investigated the competition between this mode and the $\underset{\sim}{E} \times \underset{\sim}{B}$ by solving the stability problems in similar idealized slab geometries ($K_z = 0$). Roughly speaking, the $\underset{\sim}{E} \times \underset{\sim}{B}$ goes unstable when

$$E_0 > \frac{1}{L} \frac{D_{11}^+}{\mu_{11}^+}$$

while the gravitational is unstable for

$$m_+ g > \frac{e}{L} \frac{D_\perp^+}{\mu_{11}^+}$$

* We are indebted to Dr. Francis Perkins for this observation.

Here L is roughly of the order of the characteristic length of the density gradient (although it tends to be somewhat smaller for the gravitational case). Comparing the two results above, we see that the $\underset{\sim}{E}$ X $\underset{\sim}{B}$ has the lower threshold if

$$U_o = \frac{cE_o}{B} > \frac{g}{\Omega_+}\left[1 + (\Omega\tau)_+^2\right]$$

Since $\Omega_+ \cong 24\ \text{sec}^{-1}$, $g = 9.8\text{m/sec}^2$ and U_o is of the order of 20-100 m/sec in most releases, we see that the E X B dominates by about a factor of 10 if $(\Omega\tau)_+ \cong 2$ as observations indicate. Clearly this instability is the closest contender. It must be remembered, however, that there have been releases in which the field lines were nearly vertical and which still demonstrated rapid formation of striations.

ACKNOWLEDGMENT

One of us (A.M.S.) would like to thank Mr. V. G. Abhyankar for his critical comments and for checking part of the numerical calculations.

REFERENCES

1. A. Simon, RADC-TR-70-27, February 1970. See also Jour. Geo. Res. 75, 6287 (1970). Hereafter referred to as I.
2. A. Simon, RADC-TR-70-208, September 1970. Hereafter referred to as II.

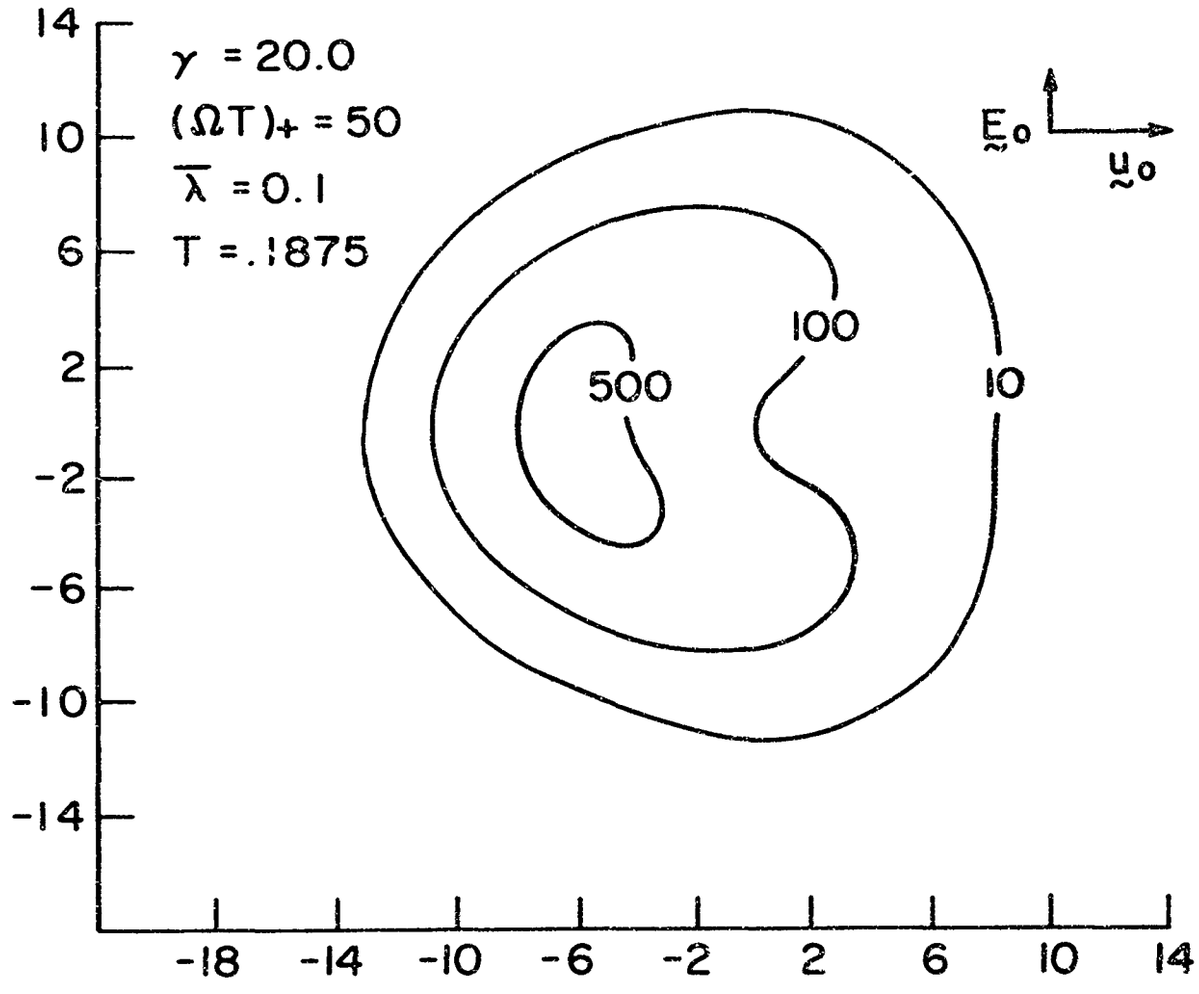

FIG. 1 DENSITY CONTOURS FOR $(\Omega T)_+ = 50$ AT $T = .1875$

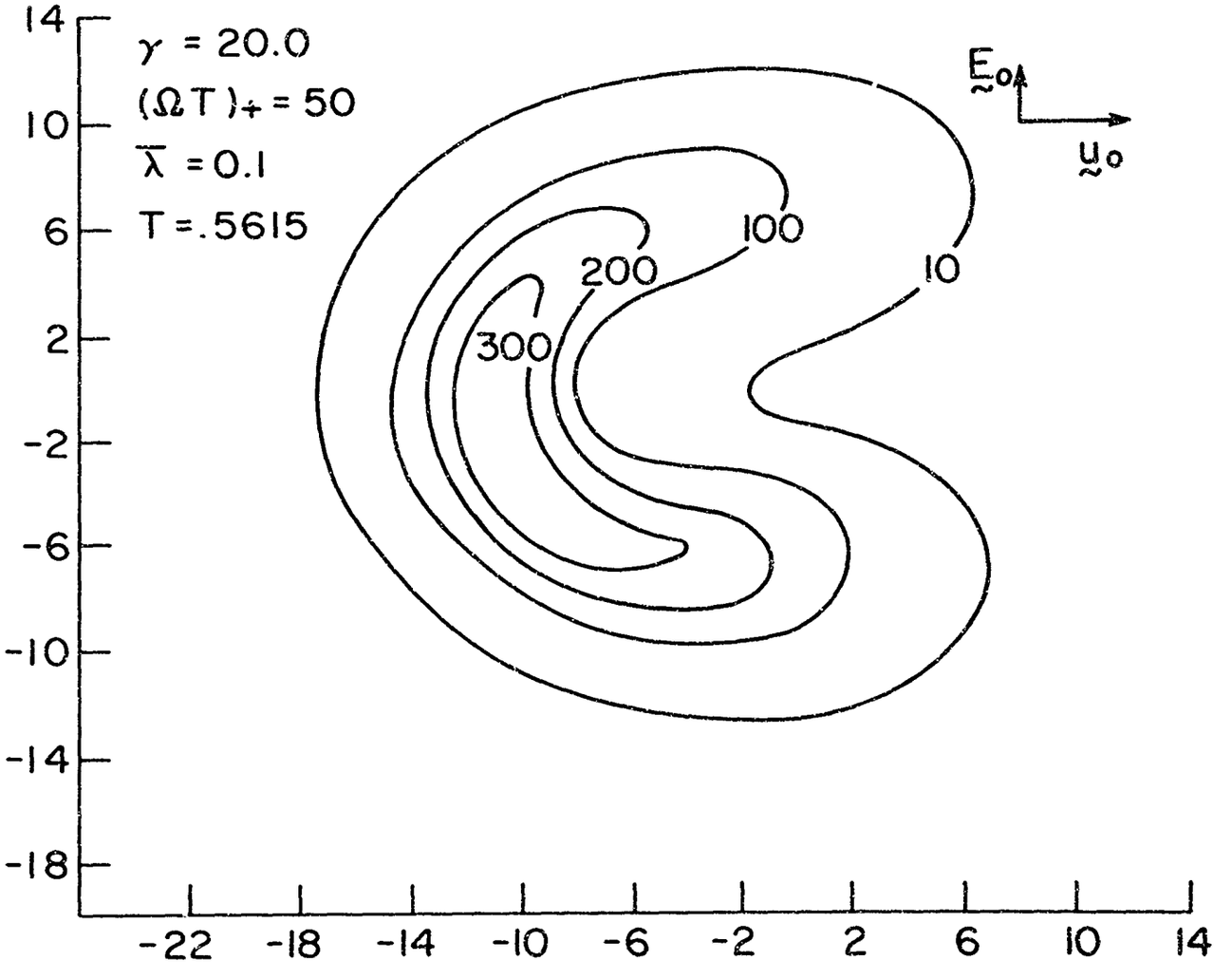

FIG. 2 DENSITY CONTOURS FOR (ΩT)+ = 50 AT T = .5615

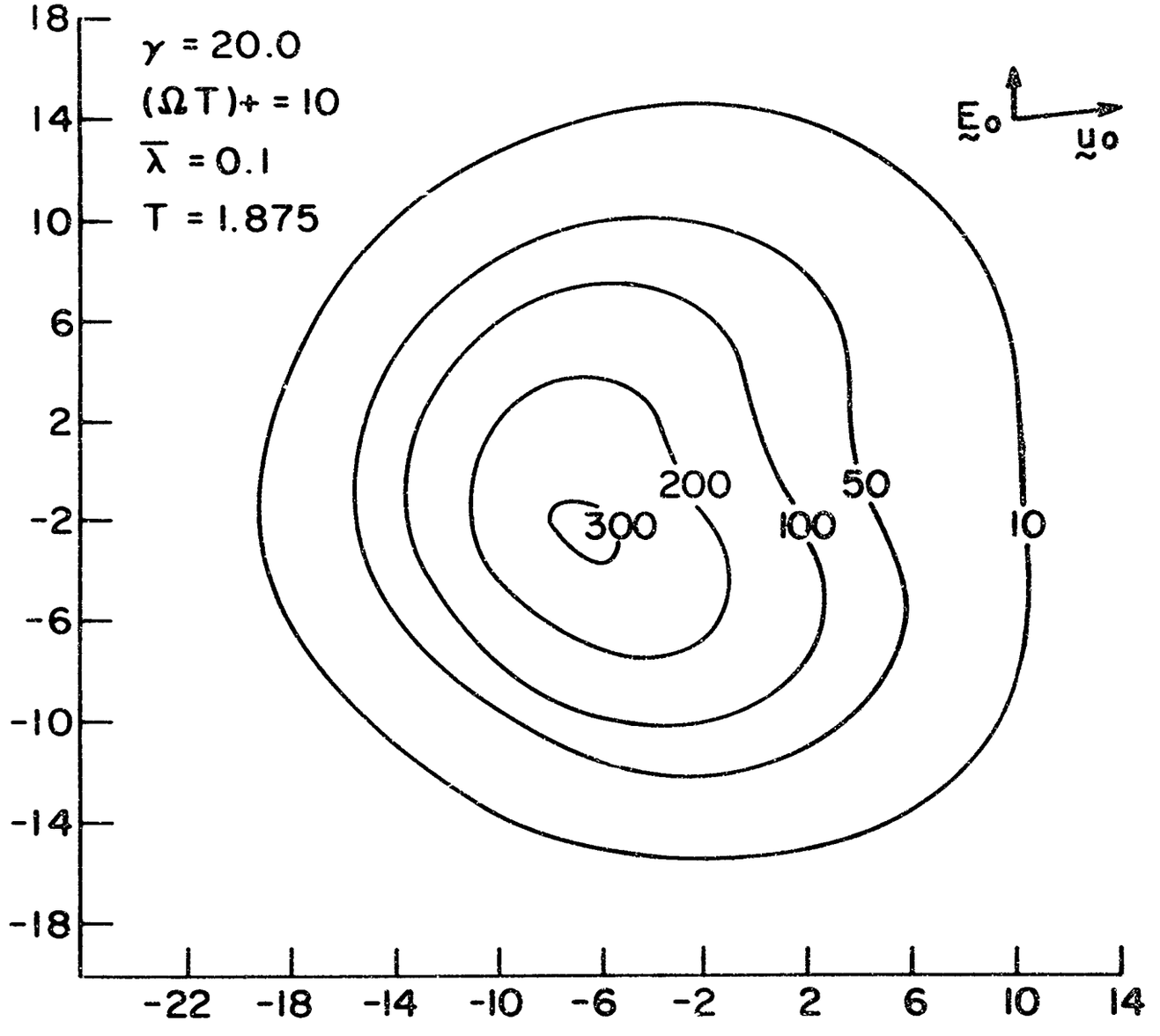

FIG. 3 DENSITY CONTOURS FOR $(\Omega T)_+ = 10.0$ AT $T = 1.875$

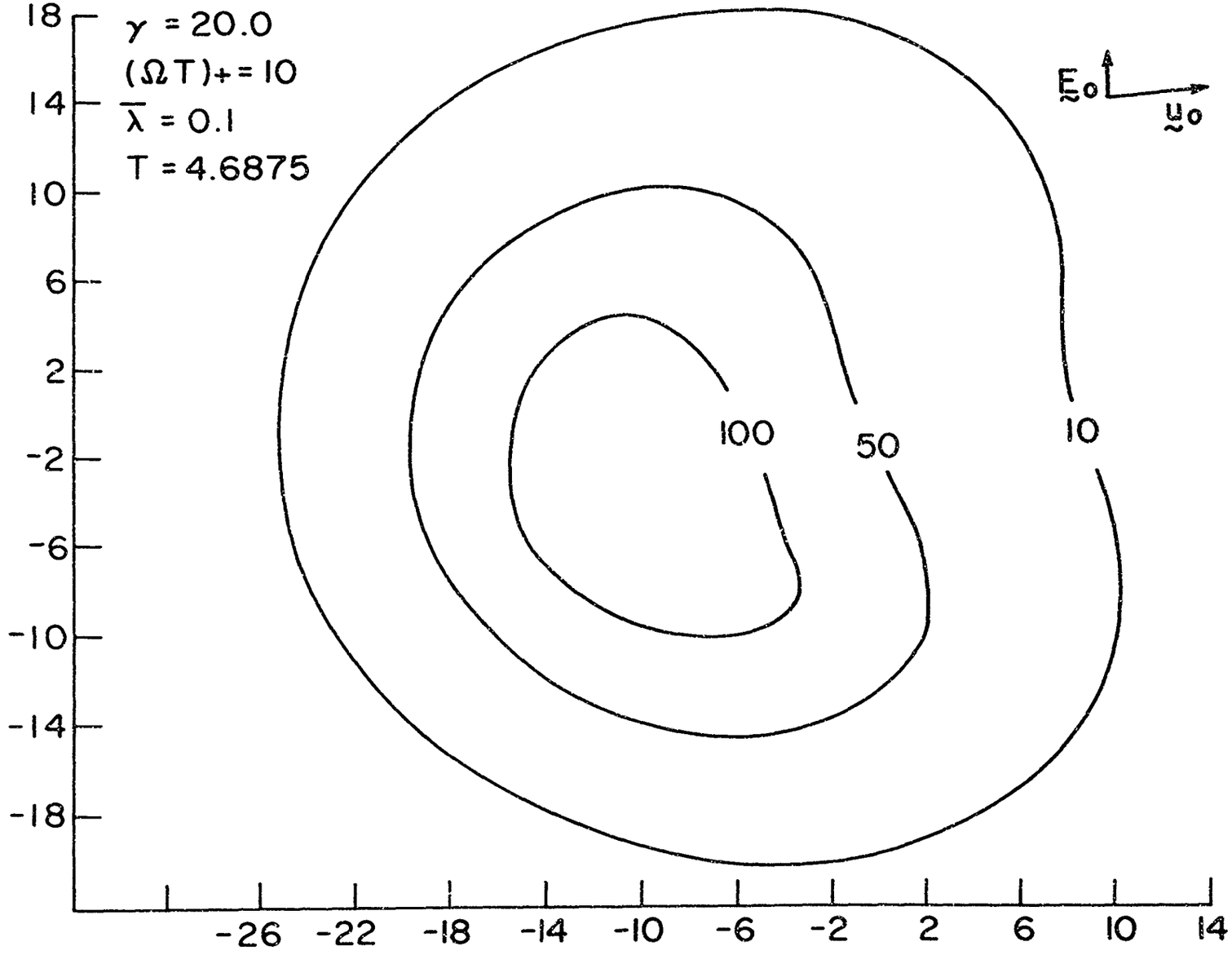

FIG. 4 DENSITY CONTOURS FOR $(\Omega T)+ = 10.0$ AT $T = 4.6875$

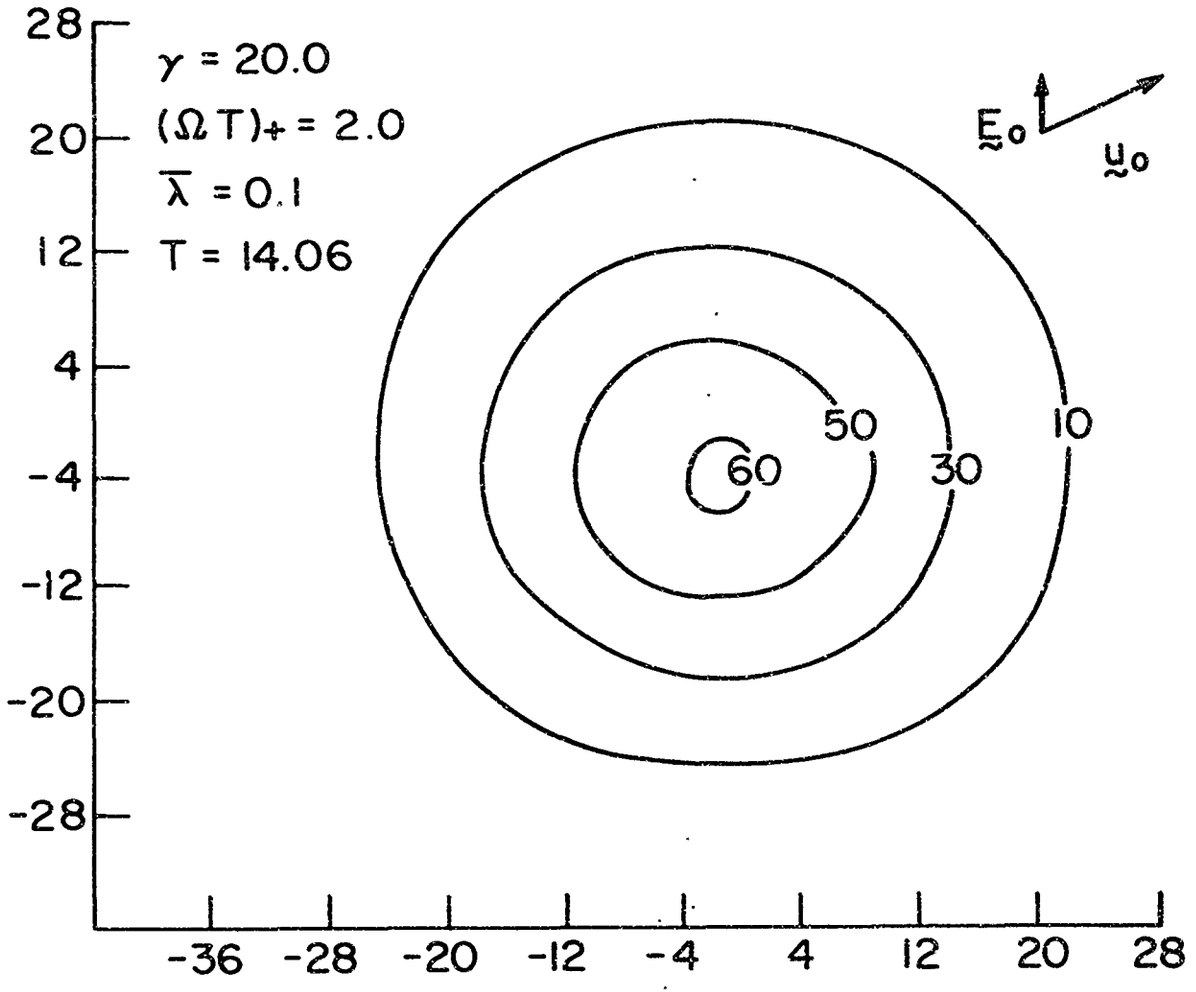

FIG. 5 DENSITY CONTOURS FOR $(\Omega T)_+ = 2.0$ AT $T = 14.06$